

Supporting Information for

**A Uranyl-Based Luminescent Dosimeter for Ultralow-Dose Tracking  
of UV and X-ray Radiation**

*Qinyan Gu<sup>a</sup>, Ji Lei<sup>b</sup>, Wenjie Deng<sup>b</sup>, Heyao Zhang<sup>a</sup>, Zhi-Hui Zhang<sup>c</sup>, Huangjie Lu<sup>c\*</sup>,  
Baowei Hu<sup>b</sup>, Jian Xie<sup>b\*</sup>*

*<sup>a</sup> Wang Zheng School of Microelectronics, Changzhou University, Changzhou, 213164, China.*

*<sup>b</sup> School of Life and Environmental Sciences, Shaoxing University, Shaoxing, 312000, China.*

*E-mail: [jxie@usx.edu.cn](mailto:jxie@usx.edu.cn)*

*<sup>c</sup> Jiangsu Key Laboratory of Advanced Catalytic Materials and Technology, Changzhou  
University, Changzhou, 213164, China. E-mail: [13913505904@163.com](mailto:13913505904@163.com)*

## Table of Content

S1. Experimental Section.....	4
S1.1 Materials and Synthesis .....	4
S1.2 Characterizations .....	4
S2. Supplementary Figures and Tables.....	6
Fig. S1. PXRD pattern of as-synthesized U-OX-PIP compared with the simulated one. ....	6
Fig. S2. SEM-EDS and mapping analysis of U-OX-PIP.....	6
Fig. S3. Photoluminescence spectra of piperazine and U-OX-PIP under 365 nm UV excitation.....	7
Fig. S4. The fluorescence lifetime of U-OX-PIP before and after 12 J/cm <sup>2</sup> UV irradiation. ....	7
Fig. S5. The $I_0/I$ ratio of U-OX-PIP as a function of UV dose. ....	8
Fig. S6. The $I_0/I$ ratio of U-OX-PIP as a function of X-ray dose. ....	8
Fig. S7. The $I_{SE}$ of (a) UV and (b) X-ray irradiation. ....	9
Fig. S8. Electron paramagnetic resonance spectra of oxalic acid before and after UV irradiation.....	9
Fig. S9. Electron paramagnetic resonance spectra of piperazine before and after UV irradiation.....	10
Fig. S10. The luminescence spectra before irradiation, after UV irradiation, and after being stored in dark for 1, 5, 15, 24, 72, 96 and 120 h. ....	10
Fig. S11. Thermogravimetric curve of U-OX-PIP.....	11
Fig. S12. Reversibility of fluorescence upon heating at 100 ° C for 48 hours.....	11
Fig. S13. The theoretical and experimental powder diffraction patterns of U-OX-PIP before and after irradiation with (a) UV and (b) X-ray.....	12
Fig. S14. The FTIR spectra of U-OX-PIP before and after irradiation with (a) UV and (b) X- ray. ....	12
Fig. S15. The PXRD patterns of U-OX-PIP before and after exposure to 50%, 70%, and 90% relative humidity for 24 h. ....	13
Table S1. Crystallographic data for U-OX-PIP.....	13
Table S2. Selected bond lengths and bond angles of U-OX-PIP.....	14

Table S3. Comparison of LODs toward UV and X-ray between U-OX-PIP and other uranyl-based materials.....14

S3. References.....15

## S1. Experimental Section

### S1.1 Materials and Synthesis

**Caution!** All uranium compounds used in these studies contained depleted uranium; standard precautions were performed for handling radioactive materials, and all studies were conducted in a laboratory dedicated to studies on actinide elements.

**Materials.**  $\text{UO}_2(\text{NO}_3)_2 \cdot 6\text{H}_2\text{O}$ ,  $\text{H}_2\text{C}_2\text{O}_4 \cdot 2\text{H}_2\text{O}$  (oxalic acid, donated as  $\text{H}_2\text{OX}$ ) and  $\text{C}_4\text{H}_{10}\text{N}_2$  (piperazine) (AR,  $\geq 99.5\%$ , Sinopharm Chemistry Reagent Co., Ltd) were used as received from commercial suppliers without further purification.

**Synthesis.** A mixture of  $\text{UO}_2(\text{NO}_3)_2 \cdot 6\text{H}_2\text{O}$  (0.0502 g, 0.1 mmol),  $\text{H}_2\text{C}_2\text{O}_4 \cdot 2\text{H}_2\text{O}$  ( $\text{H}_2\text{OX}$ ) (0.1890 g, 1.5 mmol), piperazine (PIP) (0.02 g, 0.23 mmol), and deionized water (5  $\mu\text{L}$ ) were loaded into a 10 mL glass vial. The vial was sealed and heated to 120°C for 24 h and then cooled to room temperature for 12 h. Yellowish block single crystals of **U-OX-PIP** were isolated. The crystals were washed with ethanol and dried under ambient conditions.

### S1.2 Characterizations

**Crystallographic Analysis.** The data were collected at 296 K using a Turbo X-ray Source (Mo  $K\alpha$  radiation,  $\lambda = 0.71073 \text{ \AA}$ ) adopting the direct-drive rotating anode technique and a CMOS detector. Crystals were mounted on Cryoloops with Paratone oil and optically aligned on a Bruker D8-Venture single-crystal X-ray diffractometer equipped with a digital camera. The structure was solved by Intrinsic Phasing with *ShelXT* <sup>[1]</sup> and refined with *ShelXL* <sup>[2]</sup> using *OLEX2* <sup>[3]</sup>. All non-hydrogen atoms were refined with anisotropic displacement parameters and the carbon-bound hydrogen atoms were introduced at calculated positions. Crystal data and structure refinement parameters are given in Table 1.

**Powder X-ray diffraction (PXRD).** Powder patterns were collected from 5 to 50°, with a step of 0.02° on a Bruker D8 advance X-ray diffractometer with Cu  $K\alpha$  radiation ( $\lambda = 1.54056 \text{ \AA}$ ) equipped with a Lynxeye one-dimensional detector.

**Photoluminescence Spectroscopy.** Single photoluminescence spectroscopy data were recorded from single crystals of **U-OX-PIP** using a Craic Technologies microspectrophotometer. Crystals were placed on quartz slides, and the data were collected

after optimization of the microspectrophotometer. Powder photoluminescence spectroscopy data were recorded using an Edinburgh FLS920 steady state fluorimeter with a time-correlated single-photon counting (TCSPC) spectrometer and a LED lamp as the excitation source. The UV irradiation was performed using the built-in UV excitation source of the microspectrophotometer (365 nm, 82.25 mW cm<sup>-2</sup> s<sup>-1</sup>). The X-ray radiation was provided by a W K $\alpha$  radiation source (60 kV, 1.2 Gy min<sup>-1</sup>).

**Fourier Transform Infrared (FTIR) Spectroscopy.** The FTIR spectra were recorded using a FTIR spectrometer (Thermo Nicolet 6700 spectrometer) equipped with a diamond attenuated total reflectance (ATR) accessory in the range of 400–4000 cm<sup>-1</sup>.

**Scanning Electron Microscopy and Energy-Dispersive Spectroscopy (SEM-EDS).** Scanning electron microscopy (SEM) images and energy-dispersive spectroscopy (EDS) analysis data were collected on a Zeiss Merlin Compact LEO 1530 VP scanning electron microscope with the energy of the electron beam being 15 kV. Crystals were mounted directly on the carbon conductive tape and the spectra acquisition time was 60s.

**Thermogravimetric Analysis (TGA).** TGA was carried out on a NETZSCH STA 449 F3 Jupiter instrument in the range of 30–900 °C under a nitrogen flow at a heating rate of 10 °C/min.

**Electron Paramagnetic Resonance (EPR) Study.** The EPR spectra for nonirradiated and irradiated samples was recorded on a JEOL-FA200 spectrometer. An X-band spectrometer (JES-FA200) with 100-kHz field modulation was interfaced with a computer to manipulate the spectra and integrate spectral intensity EPR measurements were performed at room temperature and the microwave power used was 1.0 mW.

**Radiolytic Stability.** The radiation resistance of **U-OX-PIP** were examined by irradiating the powdery sample with UV or X-ray under ambient conditions. UV and X-ray radiations were provided by a photochemical reactor (365nm, 25W, 80 mW cm<sup>-2</sup> s<sup>-1</sup>), and a W K $\alpha$  irradiation source (60 kV, 0.2 mA, 30 Gy min<sup>-1</sup>), respectively. PXRD and FTIR study on the irradiated samples were performed to evaluate the radiation resistance of **U-OX-PIP**.

## S2. Supplementary Figures and Tables

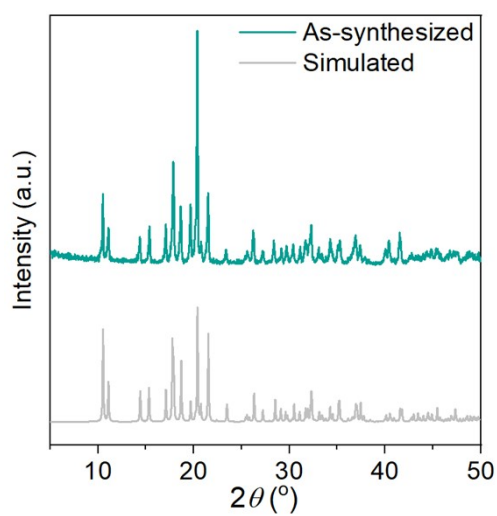


**Fig. S1.** PXRD pattern of as-synthesized U-OX-PIP compared with the simulated one.

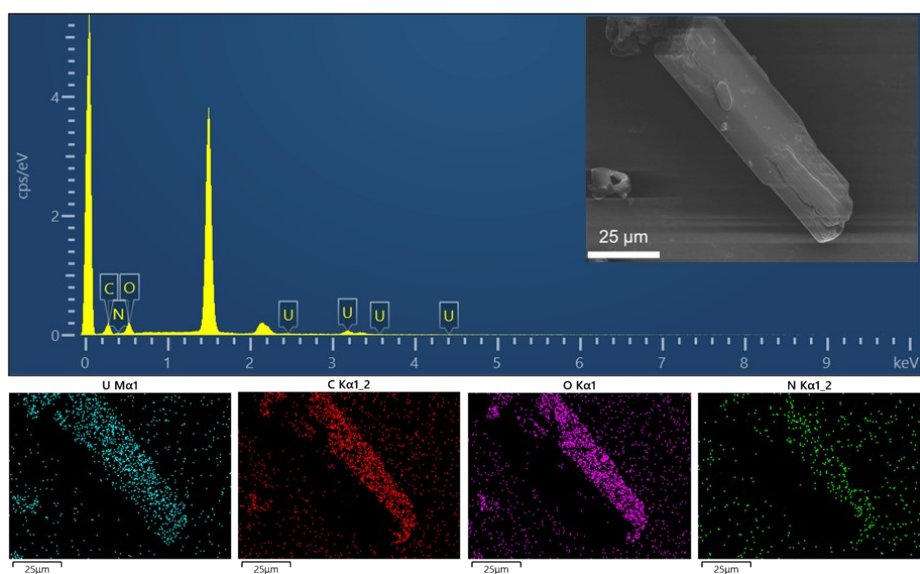


**Fig. S2.** SEM-EDS and mapping analysis of U-OX-PIP.

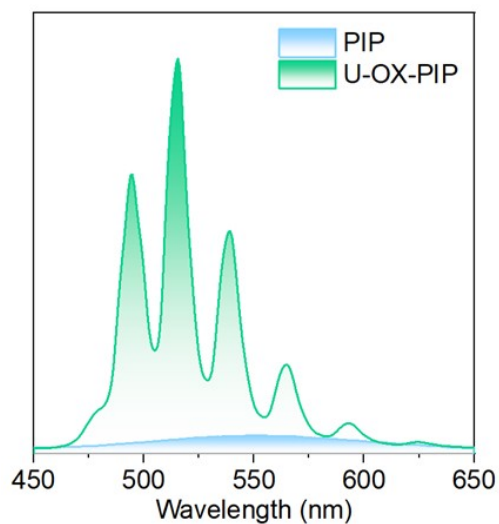


**Fig. S3.** Photoluminescence spectra of piperazine and **U-OX-PIP** under 365 nm UV excitation.

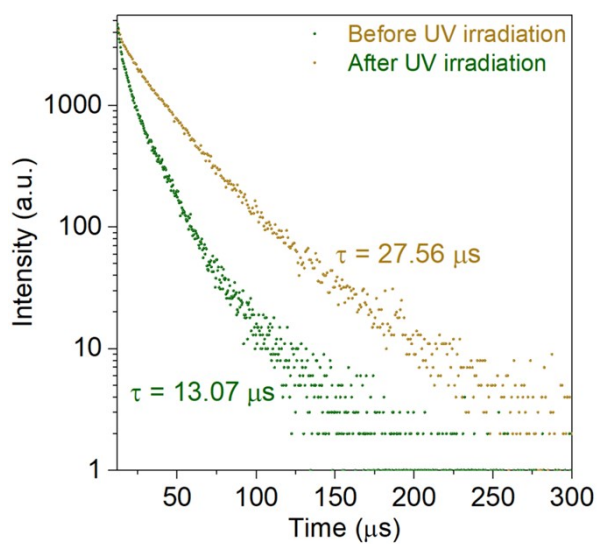


**Fig. S4.** The fluorescence lifetime of **U-OX-PIP** before and after  $12 \text{ J/cm}^2$  UV irradiation.

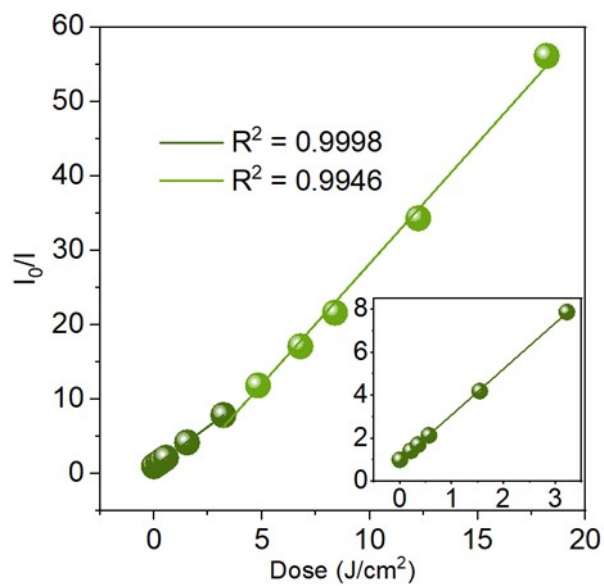


**Fig. S5.** The  $I_0/I$  ratio of **U-OX-PIP** as a function of UV dose.

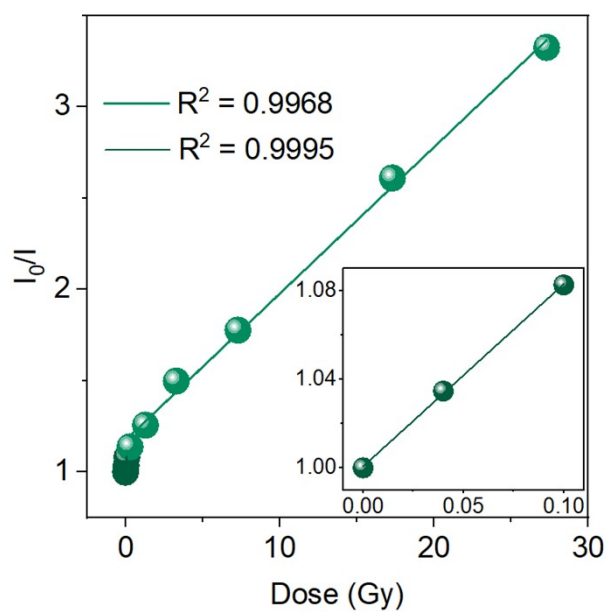


**Fig. S6.** The  $I_0/I$  ratio of **U-OX-PIP** as a function of X-ray dose.

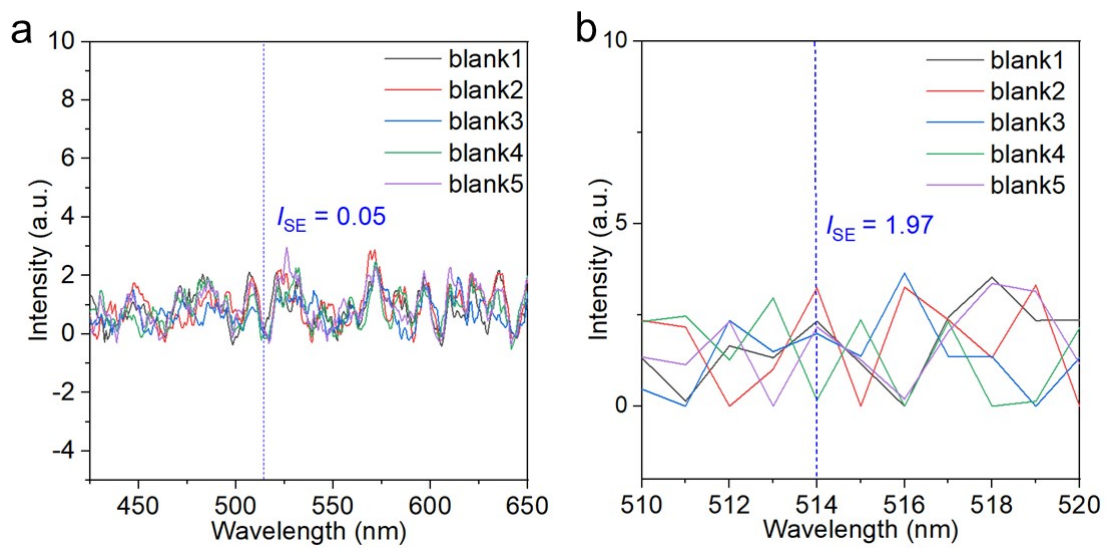


**Fig. S7.** The  $I_{SE}$  of (a) UV and (b) X-ray irradiation.

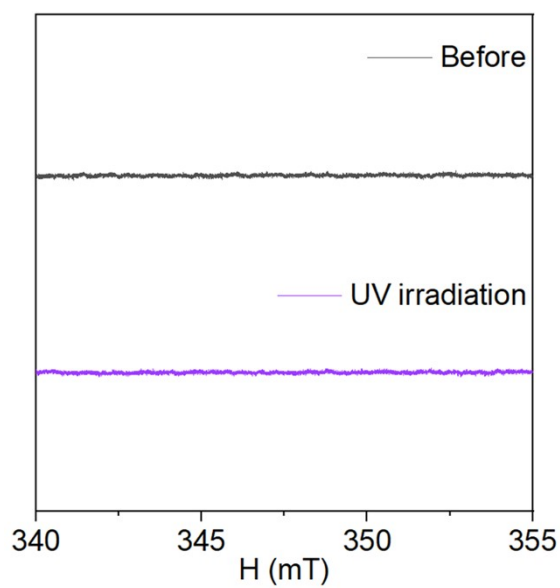


**Fig. S8.** Electron paramagnetic resonance spectra of oxalic acid before and after UV irradiation.

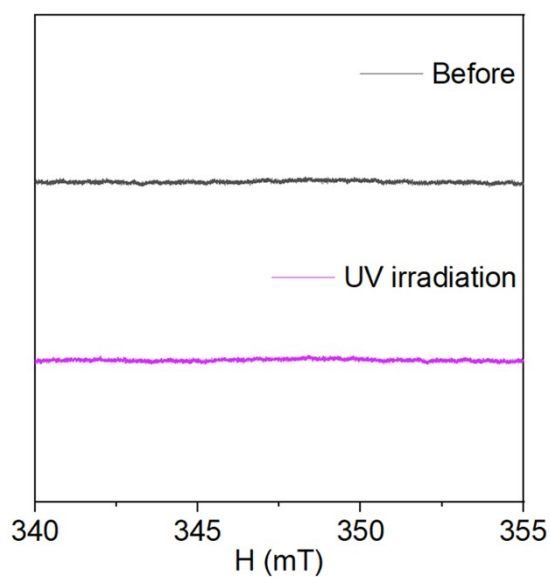


**Fig. S9.** Electron paramagnetic resonance spectra of piperazine before and after UV irradiation.

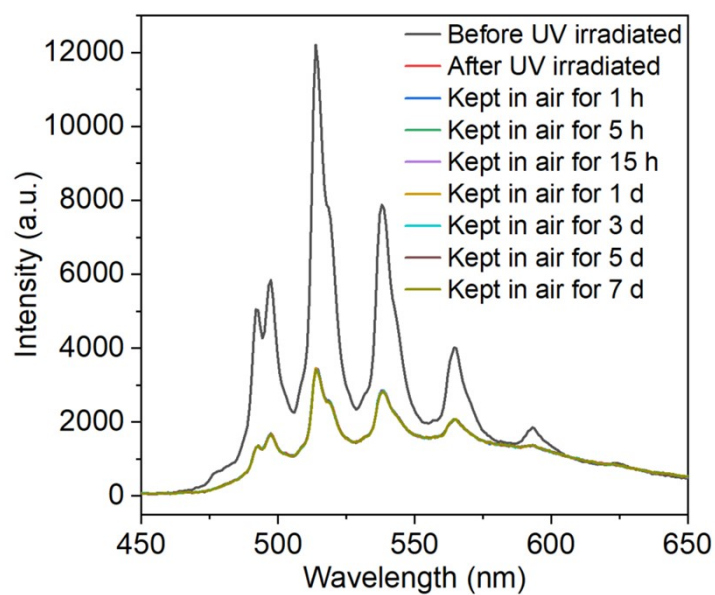


**Fig. S10.** The luminescence spectra before irradiation, after UV irradiation, and after being stored in dark for 1, 5, 15, 24, 72, 96 and 120 h.

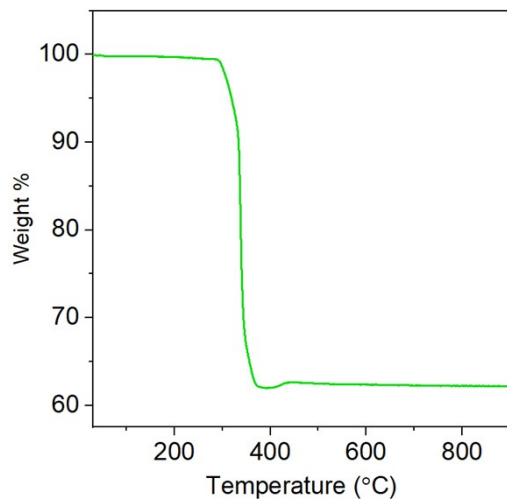


**Fig. S11.** Thermogravimetric curve of U-OX-PIP.

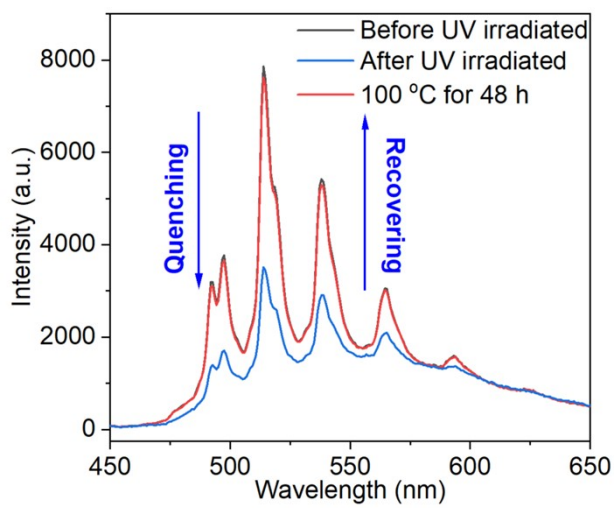


**Fig. S12.** Reversibility of fluorescence upon heating at 100 °C for 48 hours.

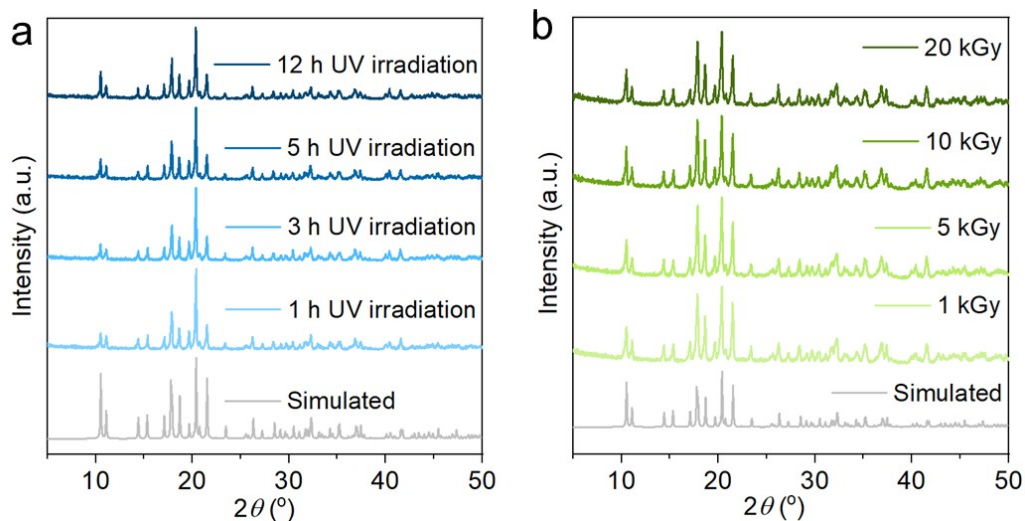


**Fig. S13.** The theoretical and experimental powder diffraction patterns of **U-OX-PIP** before and after irradiation with (a) UV and (b) X-ray.

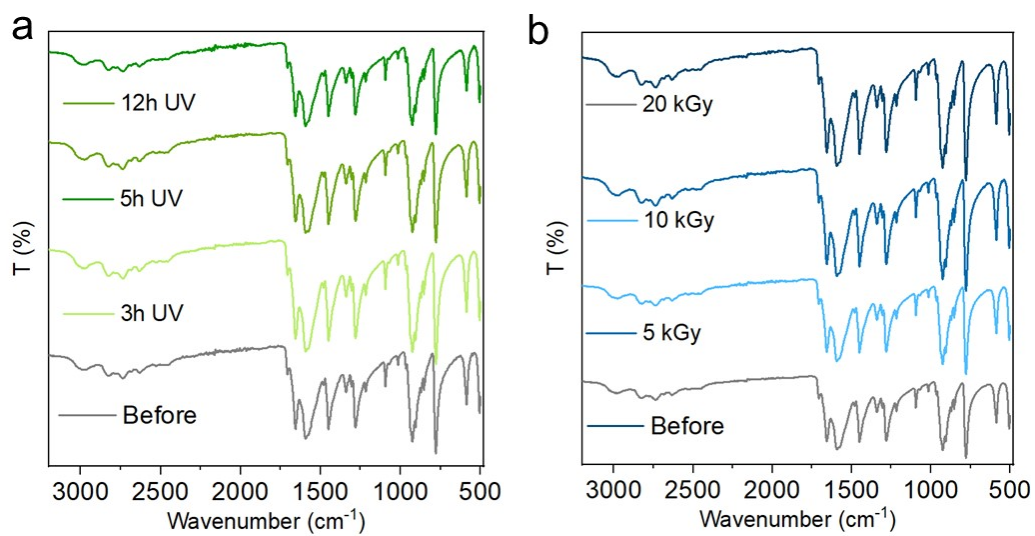


**Fig. S14.** The FTIR spectra of **U-OX-PIP** before and after irradiation with (a) UV and (b) X-ray.

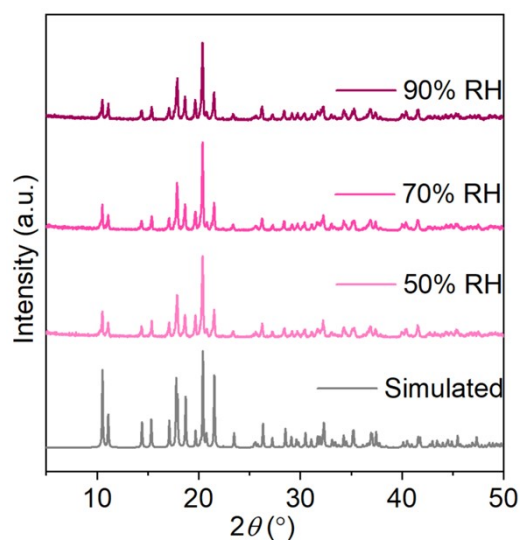


**Fig. S15.** The PXRD patterns of **U-OX-PIP** before and after exposure to 50%, 70%, and 90% relative humidity for 24 h.

**Table S1.** Crystallographic data for **U-OX-PIP**.

Compound	Before X-ray irradiation	After X-ray irradiation
<i>Mass</i>	446.13	445.13
Color	yellowish	yellowish
Habit	block	block
Space group	$P2_1/n$	$P2_1/n$
<i>a</i> (Å)	6.109(3)	6.1000(6)
<i>b</i> (Å)	16.627(7)	16.6677(17)
<i>c</i> (Å)	8.964(4)	8.9638(9)
$\alpha$ (deg)	90	90
$\beta$ (deg)	92.301(14)	92.771(3)
$\gamma$ (deg)	90	90
<i>V</i> (Å <sup>3</sup> )	909.8(7)	910.31(16)
<i>Z</i>	4	4
<i>T</i> (K)	296	296
$\lambda$ (Å)	0.71073	0.71073
<i>Max 2θ</i> (deg)	55.32	55.00
$\rho_{calcd}$ (g cm <sup>-3</sup> )	3.257	3.248
$\mu$ (Mo Ka)	0.71073	0.71073
<i>R</i> <sub>1</sub>	0.0289	0.0298
<i>wR</i> <sub>2</sub>	0.0654	0.0669
<i>Rint</i>	0.0903	0.0528
<i>GOF</i>	1.022	1.054

**Table S2.** Selected bond lengths and bond angles of **U-OX-PIP**.

	Before X-ray irradiation	After X-ray irradiation
U1=O1	1.763(5)	1.764(5)
U1=O2	1.759(5)	1.752(5)
U1–O3	2.391(4)	2.391(4)
U1–O4	2.406(4)	2.405(4)
U1–O5	2.388(4)	2.383(4)
U1–O7	2.402(4)	2.393(5)
U1–O8	2.429(4)	2.421(5)
C3–O7	1.253(7)	1.260(8)
C3–O8	1.265(7)	1.240(8)
∠O2=U1=O1	179.3(2)	179.6(2)

**Table S3.** Comparison of LODs toward UV and X-ray between **U-OX-PIP** and other uranyl-based materials.

	UV	X-ray	Ref.
<b>U-OX-PIP</b>	<b><math>8.87 \times 10^{-9}</math> J equivalent</b> to $8.87 \times 10^{-5}$ J/cm <sup>2</sup>	<b><math>8.61 \times 10^{-5}</math> Gy</b>	This work
UO <sub>2</sub> (ox)(H <sub>2</sub> O)·2H <sub>2</sub> O	N/A	<b><math>1.18 \times 10^{-5}</math> Gy</b>	4
[Hphen] <sub>2</sub> [(UO <sub>2</sub> ) <sub>2</sub> (ox) <sub>3</sub> ]	<b><math>6.9 \times 10^{-9}</math> J</b>	N/A	5
UO <sub>2</sub> (phen)(CH <sub>3</sub> COO)(OH)	$4.30 \times 10^{-6}$ J	0.32 Gy	6
UO <sub>2</sub> (5-NIPA)(DMF)	$2.4 \times 10^{-7}$ J	N/A	7
U-bppCOO	$3.26 \times 10^{-8}$ J	0.012 Gy	8
(TMA) <sub>2</sub> [(UO <sub>2</sub> ) <sub>4</sub> (ox) <sub>4</sub> L]	N/A	$5.2 \times 10^{-4}$ Gy	9
U-Cbdcp	N/A	0.093 Gy	10

### S3. References

- [1] G. M. Sheldrick, *Acta Crystallographica Section A: Found. Adv.*, 2015, **71**, 3.
- [2] G. M. Sheldrick, *Acta Crystallogr. Sect. C: Struct. Chem.*, 2015, **71**, 3.
- [3] O. V. Dolomanov, L. J. Bourhis, R. J. Gildea, J. A. K. Howard, H. Puschmann, *J. Appl. Cryst.*, 2009, **42**, 339.
- [4] J. Xie, Y. Wang, W. Liu, C. Liang, Y. Zhang, L. Chen, D. Sheng, Z. Chai and S. Wang, *Sci.China Chem.*, 2020, **63**, 1608.
- [5] J. Xie, Y. Wang, D. Zhang, C. Liang, W. Liu, Y. Chong, X. Yin, Y. Zhang, D. Gui, L. Chen, W.Tong, Z. Liu, J. Diwu, Z. Chai and S. Wang, *Chem. Commun.*, 2019, **55**, 11715.
- [6] H. Lu, Z. Zheng, J. Qiu, Y. Qian, J.-Q. Wang and J. Lin, *Dalton Trans.*, 2022, **51**, 3041.
- [7] W. Liu, X. Dai, J. Xie, M. A. Silver, D. Zhang, Y. Wang, Y. Cai, J. Diwu, J. Wang, R. Zhou, Z.Chai and S. Wang, *ACS Appl. Mater. Interfaces*, 2018, **10**, 4844.
- [8] M. Xu, H. Lu, C. Wang, J. Qiu, Z. Zheng, Z.-H. Zhang, X. Guo, M.-Y. He, J. Qian, and J. Lin, *Chem. Commun.*, 2022, **58**, 9389.
- [9] J. Xie, Y. Wang, W. Liu, X. Yin, L. Chen, Y. Zou, J. Diwu, Z. Chai, T. E. Albrecht-Schmitt, G.Liu and S. Wang, *Angew. Chem. Int. Ed.*, 2017, **56**, 7500.
- [10] Z. Zheng, J. Qiu, H. Lu, J.-Q. Wang and J. Lin, *RSC Adv.*, 2022, **12**, 12878.